IMPACT MODELING WITH SMOOTH PARTICLE HYDRODYNAMICS

R. F. STELLINGWERF and C. A. WINGATE

Los Alamos National Laboratory, MS F645, Los Alamos, NM 87545

ABSTRACT

Smooth Particle Hydrodynamics (SPH) can be used to model hypervelocity impact phenomena via the addition of a strength of materials treatment. SPH is the only technique that can model such problems efficiently due to the combination of 3-dimensional geometry, large translations of material, large deformations, and large void fractions for most problems of interest. This makes SPH an ideal candidate for modeling of asteroid impact, spacecraft shield modeling, and planetary accretion. In this paper we describe the derivation of the strength equations in SPH, show several basic code tests, and present several impact test cases with experimental comparisons.

PHILOSOPHY OF SPH

SPH is a gridless Lagrangian hydrodynamic computational technique. With some care, it can be written in a fully conservative form. The form of the SPH equations is extremely simple, even in 3 dimensions. These characteristics, together with the physical "feeling" for the problem that is embodied in a fully Lagrangian code makes SPH an attractive approach for problems with complicated geometry, large void areas, fracture, or chaotic flow fields.

SPH was first derived by Lucy (1977) as a Monte-Carlo approach to solving the hydrodynamic time evolution equations. Subsequently, Monaghan and co-workers (Monaghan 1982, 1985, 1988, Gingold and Monaghan 1977, 1982) reformulated the derivation in terms of an interpolation theory, which was shown to better estimate the error scaling of the technique. According to the interpolation derivation, each SPH "particle" represents a mathematical interpolation point at which the fluid properties are known. The complete solution is obtained at all points in space by application of an interpolation function. This function is required to be continuous and differentiable. Gradients that appear in the flow equations are obtained via analytic differentiation of the smooth, interpolated functions. Monaghan showed that other well known techniques, such as PIC, finite element, and finite volume methods could also be derived in this way through appropriate choice of interpolation technique. SPH is distinguished by the simplicity of its approach: interpolation is done by summing over "kernels" associated with each particle. Each kernel is a spherically symmetric function centered at the particle location and generally resembling a Gaussian in shape. The order of accuracy of the interpolation (and thus of the difference equations) is determined by the smoothness of the kernel. The kernel is required to approach a delta function in the limit of small extent. The interpolation is accomplished by summing each equation or variable at any location over nearby known values at particle locations, each weighted by its own kernel weighting function. Each kernel function is required to integrate over all space to exactly unity, thus normalizing the interpolation sums. By appropriately modifying the normalization condition, the same code can easily switch between 1D, 2D,

3D, spherical or cylindrical geometric configurations. This feature allows code development in 1D or 2D, with confidence that the same coding will work for all cases if implemented carefully.

There are two SPH codes currently under development at Los Alamos National Laboratory (LANL). The first is SPHC, which was originally written by Stellingwerf. SPHC is a research tool written in C that runs on a variety of platforms. The second code is SPHINX, which is a fully vectorized CRAY version with a more convenient user interface and an integrated X-Windows graphic runtime display. SPHINX will be the production code used for high resolution 2D and 3D modeling. SPHINX is currently being developed by Wingate at LANL. The code description and applications discussed below were all run on SPHC, but the coding and results from SPHINX are similar.

Applications that have been tested on these codes include blast wave stability, laser-plasma interaction, Rayleigh-Taylor instability, strong shocks, and hypervelocity impact. In the following sections we briefly discuss the equations solved in SPH, and show several hypervelocity test cases.

FLUID EQUATIONS

SPHC solves the general fluid dynamics equations. The first of these is the continuity equation

$$\frac{d\rho}{dt} + \rho \frac{\partial}{\partial x^\alpha} U^\alpha = 0 \tag{1}$$

where ρ is the material density and U is the material velocity. We use Greek superscripts to indicate coordinate directions with implied summation on repeated indices. Roman subscripts will be used to label particles. Summation is not implied on repeated subscripts (the summation sign must appear directly).

The second equation is the momentum equation

$$\frac{d}{dt} U^\alpha = \frac{1}{\rho} \frac{\partial}{\partial x^\beta} \sigma^{\alpha\beta} \tag{2}$$

where $\sigma^{\alpha\beta}$ is the stress tensor. This is divided into an isotropic part which is the pressure P and a traceless deviatoric stress tensor $S^{\alpha\beta}$ and is given by:

$$\sigma^{\alpha\beta} = -P\delta^{\alpha\beta} + S^{\alpha\beta}. \tag{3}$$

The final equation is the energy equation:

$$\frac{de}{dt} = \frac{1}{\rho} \sigma^{\alpha\beta} \dot{\epsilon}^{\alpha\beta} \tag{4}$$

where e is the specific internal energy and $\dot{\epsilon}$ is the strain rate tensor given by

$$\dot{\epsilon}^{\alpha\beta} = \frac{1}{2} \left(\frac{\partial}{\partial x^\beta} U^\alpha + \frac{\partial}{\partial x^\alpha} U^\beta \right) \tag{5}$$

Using the definition of the stress tensor (equation 3) and that the trace of the strain rate tensor is the divergence of the velocity, the energy equation can be rewritten (in perhaps the more familiar form) as:

$$\frac{de}{dt} = -\frac{P}{\rho} \frac{\partial}{\partial x^\alpha} U^\alpha + \frac{1}{\rho} S^{\alpha\beta} \dot{\epsilon}^{\alpha\beta}. \tag{6}$$

1118

The procedure for converting the analytic equations into interpolated SPH equations is described in many places, for example see Monaghan (1988) or Benz (1989). Here we list the results. The continuity equation is usually solved in integral form as:

$$\rho_i = \sum_j m_j W_{ij} \qquad (7)$$

where m_j is the mass of particle j and W_{ij} is the smoothing kernel. The kernel could be written as $W_{ij}(|r_i - r_j|, h)$ to indicate its dependence on the distance between particles i and j and its dependence on the smoothing length h. For simplicity, however, we will write it simply as W_{ij}. The smoothing length is a measure of the width of the kernel, and may vary from particle to particle. The kernel in SPHC used in these calculations is a cubic B-spline designated as W4 in Gingold and Monaghan (1982).

The momentum equation in the SPH approximation becomes:

$$\frac{d}{dt} U_i^\alpha = \sum_j m_j \left(\frac{\sigma_i^{\alpha\beta}}{\rho_i^2} + \frac{\sigma_j^{\alpha\beta}}{\rho_j^2} \right) \frac{\partial W_{ij}}{\partial x^\beta} . \qquad (8)$$

If this equation is multiplied by m_i we see that the time derivative of the momentum is exactly symmetric in i and j thus ensuring exact conservation of both linear and angular momentum.

The energy equation in the SPH approximation is:

$$\frac{de_i}{dt} = \frac{1}{2} \sum_j m_j (U_j^\alpha - U_i^\alpha) \left(\frac{\sigma_i^{\alpha\beta}}{\rho_i^2} + \frac{\sigma_j^{\alpha\beta}}{\rho_j^2} \right) \frac{\partial W_{ij}}{\partial x_i^\beta} . \qquad (9)$$

Multiplying this equation by m_i, summing over i, and using equation 8, we can prove exact energy conservation for the full system of particles. A rearragement of terms in the energy sum formed from equation (9) produces a slightly more physical and more stable form of the energy equation, which is the form used in SPHC, and is also exactly conservative:

$$\frac{de_i}{dt} = \sum_j m_j (U_j^\alpha - U_i^\alpha) \left(\frac{\sigma_i^{\alpha\beta}}{\rho_i^2} \right) \frac{\partial W_{ij}}{\partial x_i^\beta} . \qquad (10)$$

To obtain the particle approximation for the strain rate tensor we follow Libersky and Petschek (1990) to get

$$\dot{\epsilon}_i^{\alpha\beta} = \frac{1}{2} \sum_j \frac{m_j}{\rho_j} \left((U_j^\alpha - U_i^\alpha) \frac{\partial W_{ij}}{\partial x_i^\beta} + (U_j^\beta - U_i^\beta) \frac{\partial W_{ij}}{\partial x_i^\alpha} \right) . \qquad (11)$$

ELASTIC PERFECTLY PLASTIC STRENGTH MODEL

The strength model installed in SPHC is a basic Hooke's law model where the stress deviator rate is proportional to the strain rate. This type of model was first used in a smooth particle hydrodynamic code by Libersky and Petschek (1990). The elastic constitutive equation which relates the deviatoric stress rate to the strain rate can be found in various places, and is given by

$$\frac{d}{dt} S^{\alpha\beta} = 2\mu (\dot{\epsilon}^{\alpha\beta} - \frac{1}{3} \delta^{\alpha\beta} \dot{\epsilon}^{\gamma\gamma}) + S^{\alpha\gamma} R^{\beta\gamma} + S^{\gamma\beta} R^{\alpha\gamma} \qquad (12)$$

where μ is the shear modulus, and R is the rotation rate tensor defined by

$$R^{\alpha\beta} = \frac{1}{2} \left(\frac{\partial}{\partial x^\beta} U^\alpha - \frac{\partial}{\partial x^\alpha} U^\beta \right) . \qquad (13)$$

The SPH approximation to the rotation rate tensor is identical to the SPH approximation for the strain rate tensor with the plus sign is replaced by a minus sign

$$R_i^{\alpha\beta} = \frac{1}{2}\sum_j \frac{m_j}{\rho_j}\left((U_j^\alpha - U_i^\alpha)\frac{\partial W_{ij}}{\partial x_i^\beta} - (U_j^\beta - U_i^\beta)\frac{\partial W_{ij}}{\partial x_i^\alpha}\right). \tag{14}$$

The von Mises yield criterion is used for plastic flow. This criterion limits the deviatoric stress in the following way. Define a quantity f by

$$f = min\left(\left(\frac{Y_0^2}{3J}\right)^{1/2}, 1\right) \tag{15}$$

where Y_0 is the yield stress and J is the second invariant of the deviatoric stress tensor

$$J = \frac{1}{2}S^{\alpha\beta}S^{\alpha\beta}. \tag{16}$$

The deviatoric stress tensor is then limited by

$$S^{\alpha\beta} = fS^{\alpha\beta}. \tag{17}$$

PHYSICS AND MATERIAL PROPERTIES

Installation and testing of material property routines and data bases is currently one of the primary areas of code development for the SPH codes. Current models use a Grüneisen equation of state with a custom temperature/energy relation incorporating solid/liquid/vapor/ion phases. In addition, the codes can access the LANL SESAME material property library for all available materials. Additional equation of state options are planned.

Strength models currently implemented are: elastic-perfectly plastic, Johnson-Cook, and Steinberg-Guinan. Each model accesses its own data base of material properties. Fracture models are discussed in the following section.

Other physics installed in the SPHC code includes thermal diffusion, radiation diffusion, laser deposition, laser ablation, ideal magnetohydrodynamics, and neutron production. These capabilities are not used in the impact tests discussed below.

Numerical techniques in the SPHC code include variable smoothing length and particle division to model low density regions, arbitrary dimensionality and geometry, ghost particle boundary conditions, and interactive run-time graphics (Stellingwerf, 1990).

FRACTURE AND FRAGMENTATION MODELS

The treatment of fracture and fragmentation in a hydrocode continues to be a challenge. We distinguish here between the two concepts on a purely numerical level:

A *fracture model* refers to the way that an object "comes apart" during a numerical computation. It may involve generating new void regions, inserting new interfaces, or other procedures depending on the code characteristics. These new voids may or may not be capable of rejoining later in the calculation. The criteria for fracture may depend on stress level, stress history, strain level, strain rate, etc.

In SPH there is no need to artificially insert void regions, since the physical process of stretching a solid object will naturally produce cracks, spall, and other void regions in the course of the computation. Material properties that affect this process are 1) the yield condition for plastic flow, 2) a specified "spall strength" for each material that acts as a limit to the tensile stress that a material can support, and 3) a specified maximum "void fraction" that the material can support prior to failure. The exact functional form of each of these criteria depends on the strength model and the implementation of the fracture model. The simplest and most promising approach in SPH is simply to set the yield stress and the spall strength criteria according to an appropriate model for the material and allow the object to respond naturally to the body stresses at each point. The degree of brittleness or ductility of the material can be varied via the recipe for the variable smoothing length (less allowed variation implies more brittle material), or by decreasing the tensile forces at some level of void fraction, as measured by the local density (smaller allowed void fraction implies more brittle material). The preferred model is likely to be different for different materials. Tests of these ideas are currently in progress and will be presented in future publications.

In contrast to the numerical treatment of fracture, a *fragmentation model* is a phenomenological model of the characteristics of the debris formed from a certain type of impact. The approach of Grady and Kipp (1987) is an example of this type of model. A fragmentation model can predict the degree of damage at each point in an object for use by a fracture model, and predict the distribution of masses, shapes, etc. of debris fragments over a much wider range than the hydrocode alone. Such a model has been tested in SPH by Benz and Melosh (1992) and is currently implemented in the LANL SPH codes.

BASIC CODE TESTS

The SPH technique has been validated for a variety of simple test cases including rarefaction expansion, spherical blast wave, shock tube, and the Noh problem (infinite strength converging shock). As an illustration of the code results on such a test, we show in figure 1 the SPH solution for a Riemann shock tube with an initial density jump of a factor of 4 at a specific time for three different cases of particle resolution. An artificial viscosity is added to the pressure to handle the shock, resulting in the shock front being spread over 3-5 particles, but the solution is very close to the plotted analytic result, and is clearly converging as the resolution is increased.

As a test of the strength models, the Taylor Anvil test of an iron rod colliding at 197 m/s with an unyielding surface has been computed. Figure 2 shows the results with the simple elastic-plastic as well as the more detailed Johnson-Cook strength models. The experimental data are taken from Johnson and Holmquist (1988), and are shown as an outline in solid lines. Although both cases represent the data very reasonably, the Johnson-Cook model does a better job reproducing the spreading at the surface and the small shoulder above the spreading region. Sections of rods taken following experiments show incipient fracturing and small void regions near the bottom of the rods. Although the simulation is rather coarse resolution, the rearrangement of particles near the surface/rod interface represents this effect.
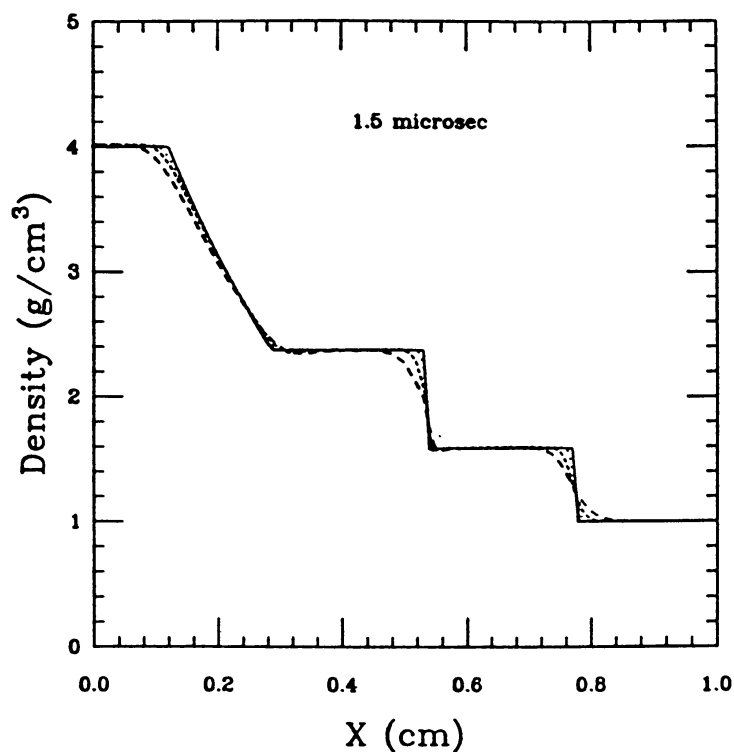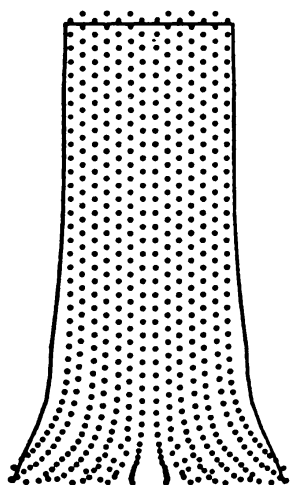
1.5 microsec

Density (g/cm^3)

X (cm)

Fig. 1. Comparison of SPH results for 90, 180, and 360 particles to the exact analytic solution for the Riemann shock tube test case with $\gamma = 1.4$, initial density jump = factor of 4

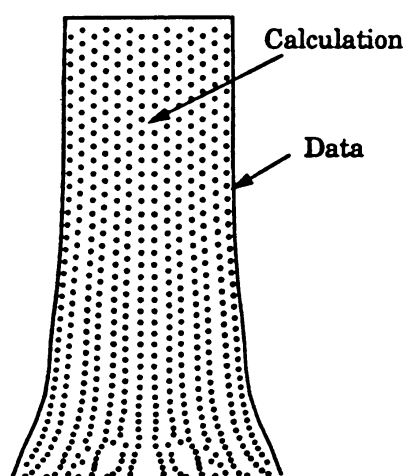Elastic Plastic   Johnson-Cook

Calculation

Data

Fig. 2. Taylor anvil tests: final configuration of an Armco Iron rod after collision with a rigid surface at 197 m/s. Left: elastic-plastic strength mod/ el, right: Johnson-Cook model. Solid line: data

THIN BUMPER SHIELD COLLISION AT 6.75 KM/S

This section describes a simulation of a spherical aluminum projectile with radius 0.475 cm colliding with a thin aluminum sheet with thickness 0.0381 cm at a velocity of 6.75 km/s. This test is similar to a very well documented series of experiments done recently by Piekutowski (1992a,b) at University of Dayton Research Institute.

This simulation was run using SPHC with about 2500 particles in 2D cylindrical mode. The EOS is Grüneisen, and the strength model is elastic/plastic. The spall strength was set to 6 kbar. Figure 3 shows the initial conditions as well as the material configuration at 5 and 10 µs. This is a particle plot, which indicates the location of the material, with a gray scale to show values of the local density. We see that the projectile has broken into many fragments with a conspicuous spall "bubble" at the rear surface, and numerous cracks along the direction of motion that have developed as a result of later expansion of the projectile. The bulk of the material lies in a flattened disk, with what appears to be an intact core. The halo of low density material in front of and to the sides of the fractured projectile is liquid/vapor material formed from the impacted bumper and a thin shell of the projectile. All of these features are consistent with experimental radiographs, although details, such as the structure in the liquid/vapor phases, do not correspond exactly. We expect that these details will improve with the planned upgrading of the equation of state.
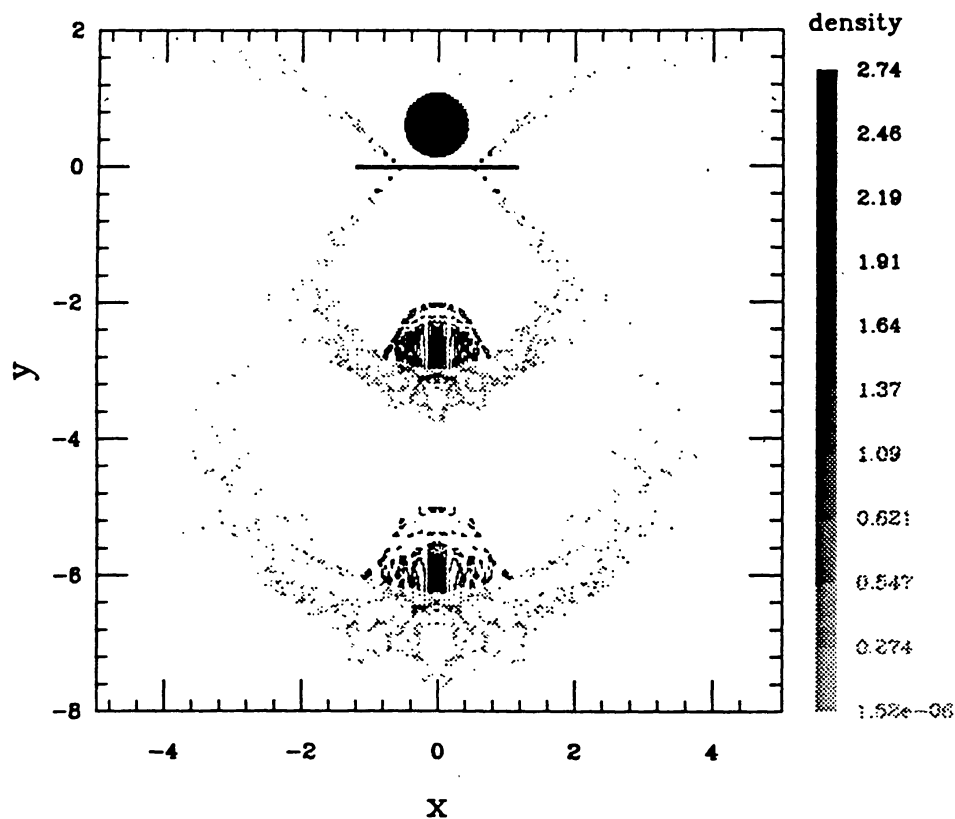

Fig. 3. Snapshots of the spherical projectile/ bumper collision at time = 0, 5, and 10 µs.

This simulation will be used as the primary test of the fracture/fragmentation scheme as the codes develop.

SHIELD / HULL COLLISIONS AT 10 KM/S.

As another example of an SPH impact application, we show models of several aluminum disk impact experiments carried out at Sandia by Chhabildas, et al. (1991).

The first model is of the experiment designated WS-12, or NASA-12. The initial setup for the run is shown in figure 4 (left). The model was run with 10,000 particles in 2D cylindrical geometry with SPHC. The EOS is Grüneisen, and the strength model is elastic/plastic. The spall strength was set to 6 kbar. The projectile is a disk of radius 0.95 cm, thickness 0.0868 cm, and velocity 10.0 km/s. The shield is a plate of thickness 0.127 cm. Both projectile and shield are made of 6061-T6 aluminum. The "hull" or witness plate was placed 11.43 cm beyond the shield, has thickness 0.32 cm, and was made of 2219-T87 aluminum. On the right of figure 4 we show the material configuration at 16 μs, just as the debris reaches the hull plate. In this case the entire cloud of debris is liquid at the vaporization temperature, indicating a mixed phase region. A dense column extends downward from the shield to the hull with nearly constant density of about 0.1 g/cc and a linear velocity profile. This column is about 1/2 projectile material and 1/2 shield material, as expected. The central core is surrounded by a halo of lower density material, extending to a shell of extruded shield at the outer edge. The maximum velocity of the debris is found to be nearly equal to the impact velocity of 10.1 km/s. This result agrees very well with UDRI experiments (Schmidt, et al. 1992, fig. 13a). A low density shell of material travelling at 14 km/s was observed in the Sandia experiment, but does not appear in this simulation.
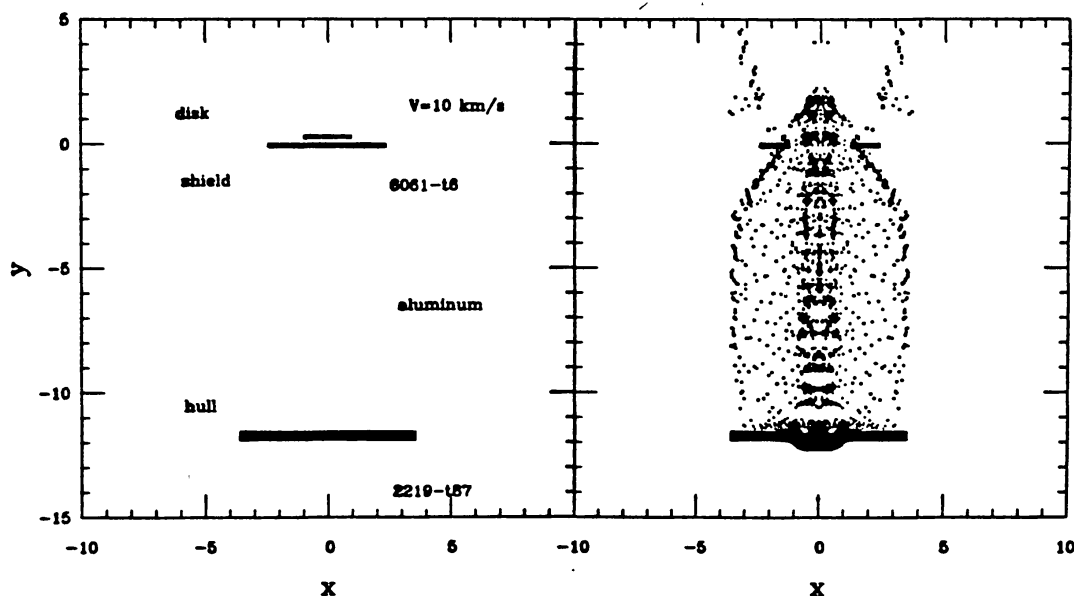

Fig. 4. Left: initial configuration for the simulation of WS-12. Right: configuration at secondary impact at 16 μs.

Figure 5 shows a details of the hull at 16 and 28 μs. At 16 μs the impacting liquid material has fully vaporized, a liquid layer has formed at the surface of the hull material, and strong hydrodynamic instability has developed at the interface. At 28 μs the hull is fully ruptured and hot vapor has begun to flow to the rear of the impact point. The times of hull deformation and rupture agree well with experiment, and both show a hole diameter of about 2 cm.
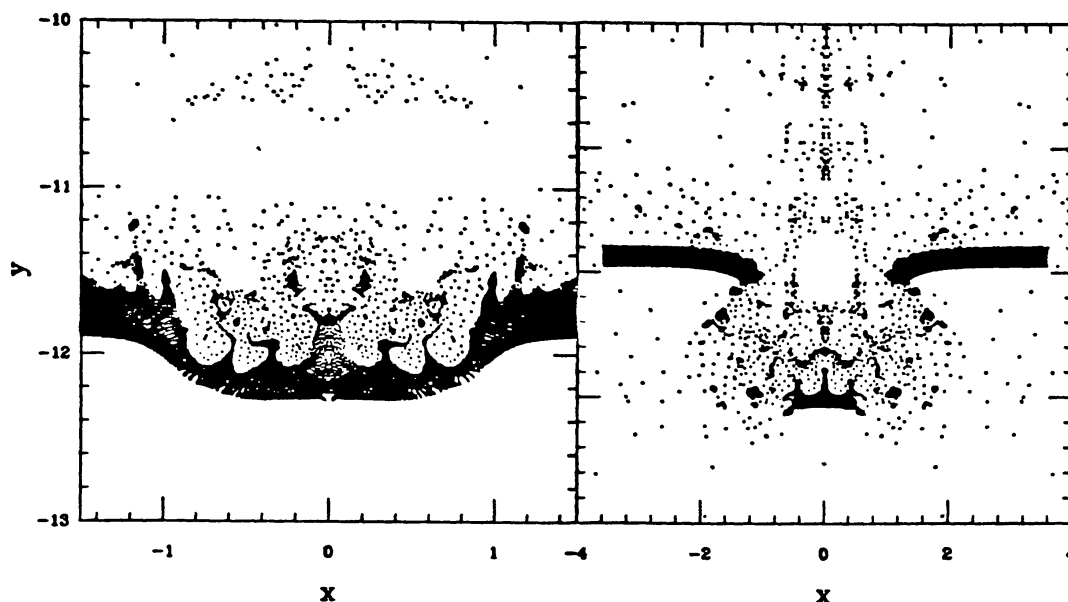
1124

Fig. 5. Detail of the hull showing development of the hole and surface insta-
bilities. Left: at 16 µs, right: at 28 µs. Note change of scale.

Another experiment, designated WS-11, or NASA-11, was also modeled. This experiment was similar to WS-12 except that the projectile radius was 0.60 cm, thickness 0.0953, and velocity 10.5 km/s. This implies about half the mass of WS-12. Shot WS-11 did not penetrate the hull, although some hull damage was observed. A model similar to the above WS-12 simulation was run with WS-11 parameters, and produced a ruptured hull similar to that observed in figure 5. Chhabildas, et al. comment that the projectile may have been distorted in some or all of the experimental shots, and this may have been the case for shot WS-11. The model was therefore re-run with a slightly "cupped" projectile, achieved by replacing the disk with a shallow cone with slope 0.25. Figure 6 shows the configuration for this simulation, again at 16 µs. In this case the hull has not ruptured, since the debris is considerably dispersed at its leading edge. The exact symmetry of the simulation, however, has formed virtually all of the projectile material into an arrow of dense material that is arrayed along the axis of the simulation, and does produce a small hole in the hull at later time. Asymmetries present in the experiment probably break up this "arrow", resulting in the several scattered damaged regions actually observed. A 3-dimensional simulation of this case is planned to test this hypothesis. The SPH results shown here are in general agreement with the CTH code results shown in Chhabildas et al. (1991).
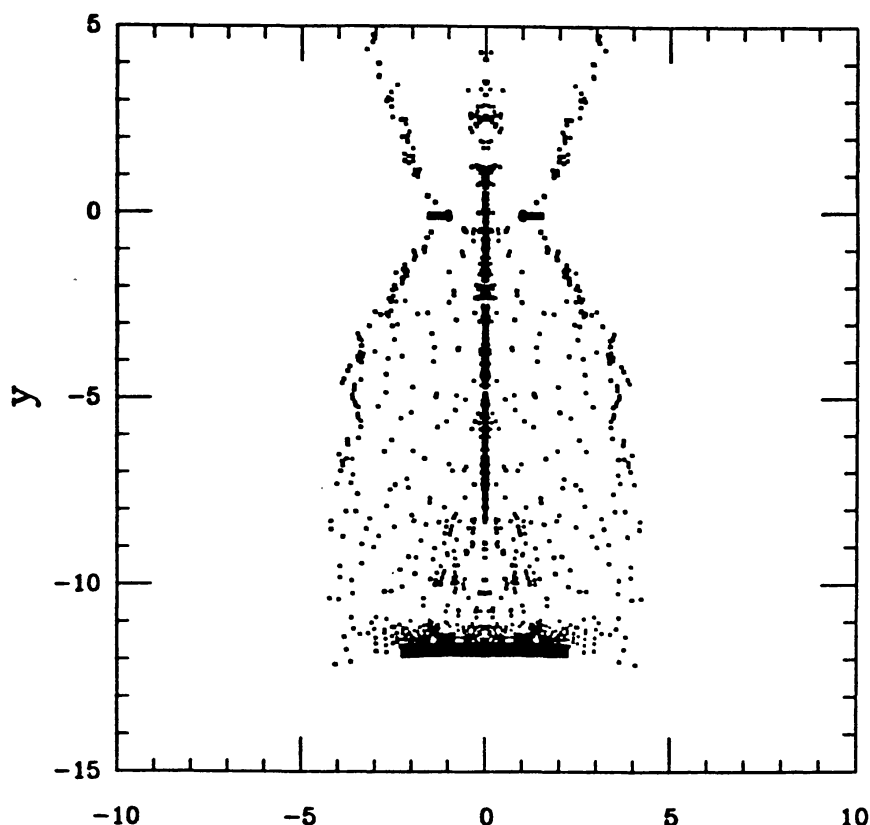
Fig. 6. The WS-11 simulation at 16 μs, showing intact hull and projectile "arrow".

OBLIQUE IMPACTS

The calculations of a sphere obliquely impacting a bumper modeled a NASA impact experiment similar to EH1C (Schonberg. et al. 1988). The sphere was made of 1100 Aluminum with a radius of 0.476 cm, a velocity of 7.0 km/s and a 60 degree angle from the normal. The bumper was 6061-T6 Aluminum with a thickness of 0.16 cm. The calculation was done in 3 dimensions using 60,000 particles. The equation of state used was Grüneisen. The strength model was elastic perfectly plastic with a shear modulus of 265 kbar and a yield strength of 0.345 kbar for the 1100 Al and 2.75 kbar for the 6061-T6 Al. The configuration after 20 microseconds is shown in Figure 4, side projection. Some projectile material scraped from the top of the projectile upon impact has slid along the plate and continued to the left, followed by ejected target material above the plane of impact. The long feature so formed is travelling ballistically to the left - there is no boundary beyond that shown in the figure. Below the plane, the projectile material is located at the left edge of the debris cloud, while target material forms the bulk of the rest of the cloud. This configuration is matched almost identically in unpublished experimental results obtained by Piekutowski at UDRI (experiment 4-1439).
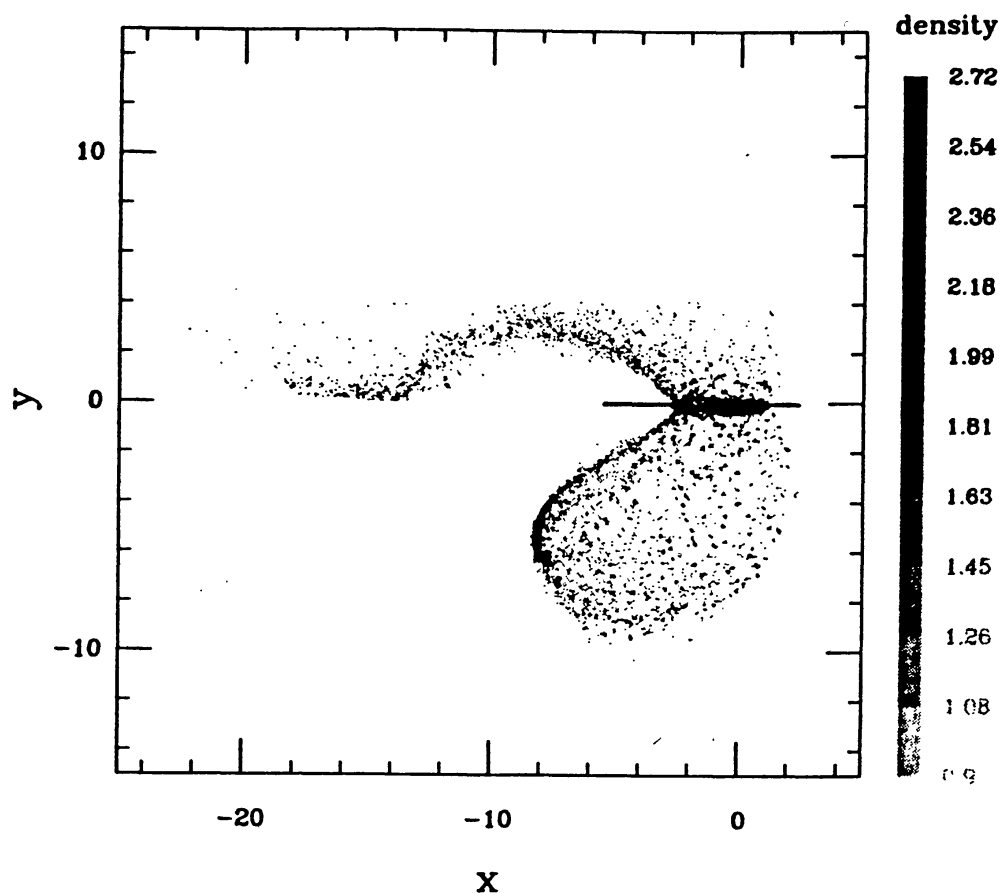
1126

Fig. 7. Oblique impact model, projectile is a sphere entering at an angle of 60 degrees from the normal moving from top right to bottom left. See text for details.

SUMMARY.

The technique of Smooth Particle Hydrodynamics shows considerable promise for simulations of hypervelocity impacts. Of special interest is its ability to produce and track debris fragments, allowing computation of secondary impacts over unlimited distances.

The SPH codes at LANL are currently undergoing tests on a variety of applications, and are in the developmental stage of code and material properties upgrades. The results so far are encouraging, and further improvements should produce a useful and unique tool

ACKNOWLEDGMENTS.

REFERENCES

Benz, W. (1989). Smooth Particle Hydrodynamics: A Review, Harvard-Smithsonian Center for Astrophysics Preprint No. 2884.

Benz W.,and H. J. Melosh, (1992) private communication.

Chhabildas, L. C., E. S. Hertel, W. D. Reinhart and J. M. Miller, (1991). Whipple Bumper Shield Results And CTH Simulations At Velocities In Excess Of 10 km/s, Sandia Technical Report SAND-91-2683.

Gingold, R. A. and J. J. Monaghan (1977). Smoothed Particle Hydrodynamics: Theory And Application To Non Spherical Stars, Mon. Not. Roy. Astron. Soc. 181, 375-389.

Gingold R. A. and J. J. Monaghan (1982). Kernel Estimates as a Basis for General Particle Methods in Hydrodynamics, J. Comput. Phys. 46, 429-453.

Grady D. E. and M. E. Kipp, (1987). Dynamic Rock Fragmentation, Fracture Mechanics of Rock, Academic Press, 429-475.

Johnson, G. R. and T. J. Holmquist (1988). Evaluation of Cylinder-impact Test Data for Constitutive Model Constants, J. Appl. Phys. 64, 3901-3910.

Libersky L. D., and A. G. Petschek, (1990). Smooth Particle Hydrodynamics with Strength of Materials, Advances in the Free-Lagrange Method, (Trease, Fritts, and Crowley, eds.), Springer Verlag, 248

Lucy, L. (1977). A Numerical Approach To Testing the Fission Hypothesis, Astron. J., 82, 1013-1024.

Monaghan, J. J. (1988). An Introduction to SPH, Comput. Phys. Comm. 48, 89-96.

Monaghan, J. J. (1982). Why Particle Methods Work, SIAM J. Sci. Stat. Comput. 3, 422-433.

Monaghan, J. J. (1985). Particle Methods for Hydrodynamics, Comp. Phy. Rep. 3, 71-124.

Piekutowski, A. (1992a). Properties of Largest Fragment Produced by Hypervelocity Impact of Aluminum Spheres with Thin Aluminum Sheets, AIAA 92-1588, Space Programs and Technologies Conference.

Piekutowski, A. (1992b). Characteristics Of Debris Clouds Produced by Hypervelocity Impact of Aluminum Spheres with Thin Aluminum Plates, this volume.

Schmidt, R. M., Housen, K. R., Piekutowski, A. J. and Poormon, K. L. (1992). Cadmium Simulations of Orbital Debris Shield Performance to 18 km/s, this volume.

Schonberg, W. P., R. A. Taylor, and J. R. Horn, (1988). An Analysis of Penetration and Ricochet Phenomena in Oblique Hypervelocity Impact, NASA TM-100319.

Stellingwerf, R. (1989). The SPH_C Manual, User's Guide, Programmer's Guide, Technical Guide, Function Reference, Test Cases, Mission Research Corporation report AMRC-N-384.1-384.5.

Stellingwerf, R. F (1989). Boundary Condition Tests Using Smooth Particle Hydrodynamics, Mission Research Corporation report MRC/ABQ-N-426.

Stellingwerf, R. F (1990). Blast Wave Stability in Nuclear Explosions I, Mission Research Corporation report MRC/ABQ-R-1254.

Stellingwerf, R. F. and R. E. Peterkin, (1990). Smooth Particle Magnetohydrodynamics, Mission Research Corporation report MRC/ABQ-R-1248.

Stellingwerf, R. F. (1990). Smooth Particle Hydrodynamics, Advances in the Free-Lagrange Method, (Trease, Fritts, and Crowley, eds.), Springer Verlag, 239.

Stellingwerf, R. F. (1992). Shock Tests for Smooth Particle Hydrodynamics, LANL memo X-1(1/92)29.

Wilkins, M. L. (1969). Calculation of Elastic-Plastic Flow, Lawrence Livermore National Laboratory report UCRL-7322 Rev. 1.

Wingate, C. A. and H. N. Fisher, (1992). Strength Modeling in SPHC, in preparation.